Agr. Nat. Resour. 57 (2023) 181–190

AGRICULTURE AND NATURAL RESOURCES

Journal homepage: http://anres.kasetsart.org

Research article

Phenazine and quinolone are main compounds produced by *Pseudomonas aeruginosa* N1 during inhibitory interaction with *Rhizopus microsporus*

Dewi Peti Virgianti[a,d,†], Dessy Natalia[c,†], I Nyoman Pugeg Aryantha[a,b,*]

[a] *School of Life Sciences and Technology, Institut Teknologi Bandung, Bandung 40132, Indonesia*

[b] *Bioscience and Biotechnology Research Centre, Institut Teknologi Bandung, Bandung 40132, Indonesia*

[c] *Biochemistry Research Division, Faculty of Mathematics and Natural Sciences, Institut Teknologi Bandung, Bandung 40132, Indonesia*

[d] *Faculty of Health Sciences, Universitas Bakti Tunas Husada, Kota Tasikmalaya 46196, Indonesia*

Article Info

Article history:
Received 20 February 2022
Revised 13 November 2022
Accepted 22 December 2022
Available online 28 February 2023

Keywords:
Antagonism,
Antifungal,
Bacterial fungal interaction (BFI),
Biocontrol,
Secondary metabolite.

Abstract

Importance of the work: *Pseudomonas aeruginosa* N1 inhibits *Rhizopus microsporus* growth by the production of quinolone, phenazine and rhamnolipid.

Objectives: To evaluate the compounds extracted from *P. aeruginosa* N1 monoculture and from co-culture between *R. microsporus* and *P. aeruginosa* N1 and to observe the degree of damage caused to *R. microsporus* by its inhibitory interaction with *P. aeruginosa* N1.

Materials & Methods: The inhibitory interaction of *P. aeruginosa* N1 was studied based on the metabolite released during *R. microsporus* inhibition. The substance released during the inhibitory interaction between *R. microsporus* and *P. aeruginosa* N1 was compared using monoculture and co-culture methods, with further analysis using liquid chromatography mass spectrophotometry (LC-MS).

Results: Based on the LC-MS analysis, quinolone, phenazine and rhamnolipid compounds were the main substances produced during the interaction between species. There was a slight difference between the detected compounds produced in monocultures and those produced in co-culture. Specifically, 2-nonyl-4-hydroxyquinoline N-oxide and mono-rhamnolipid compounds were detected only in the *P. aeruginosa* N1 monocultures. On the other hand, the compounds 2-heptyl-4-quinolone, 1-hydroxy-2-[(2E)-2-nonen-1-yl]-4 (1H)-quinolinone and 2-nonyl-3-hydroxy-4-quinolone, were detected only in co-culture.

Main finding: Quinolone, phenazine and rhamnolipid were the main compounds produced during the inhibitory interaction between *P. aeruginosa* N1 and *R. microsporus*. Furthermore, these compounds played an important role in improving antagonism against *R. microsporus*. However, this may regulate differently in each strain.

† Equal contribution.

* Corresponding author.
E-mail address: nyoman@sith.itb.ac.id (I.N.P. Aryantha)

https://doi.org/10.34044/j.anres.2023.57.1.19

Introduction

Pseudomonas aeruginosa is a phenazine-producing bacteria that can be used as a biocontrol against plant pathogenic fungi. For example, *P. aeruginosa* M18 and *P. aeruginosa* PA1201 isolated from the rhizosphere were reported as biocontrol agents. They primarily produce 1-phenazinecarboxylic acid (PCA) compounds that have been registered as environmental-friendly fungicidal products (Sun et al., 2016). PCA, commercially known as "Shenginmycin", is used to control diseases in rice and vegetables, particularly those caused by *Rhizoctonia solani* and *Fusarium oxysporum* (Xu et al., 2013). In addition, *P. aeruginosa* has been shown to inhibit other microbial growth, particularly fungi, through various mechanisms, including the release of quorum-sensing signaling compounds, siderophores, enzymes, rhamnolipids and phenazine (Chatterjee et al., 2020).

Kousser et al. (2019) reported the antibiosis mechanism of *Pseudomonas* against *Rhizopus*, with clinical samples demonstrating that *P. aeruginosa* produced siderophores that could chelate iron, thereby inhibiting the germination of *R. microsporus* spores. In agriculture, *Rhizopus* is known as a spoilage agent in some fruit and vegetables (Udoh et al., 2015), as a contaminant and spoilage agent in fresh and processed foods (Pitt and Hocking, 2009) and as a producer of mycotoxins that are harmful to humans (Jennessen et al., 2005). Furthermore, *R. microsporus* can cause disease in young rice plants by inhibiting cell division and causing abnormal swelling of the roots (Hong and White, 2004). In the medical field, *Rhizopus* causes mucormycosis in humans, particularly in immunocompromised patients (Dolatabadi et al., 2015).

The combination of physical associations and molecular communication between fungi and bacteria can produce different impacts on each organism involved. In the end, these changes can affect the fungus-bacteria complex in its biotic and abiotic environments (Frey-Klett et al., 2011). In antagonistic molecular communication, the bacteria or fungi involved in the association can produce metabolites that inhibit the growth and morphology of their interaction partners. Associated ectosymbiotic bacteria in fungi can cause damage to fungi. For example, a consortium of ectosymbiotic bacteria of the genera *Serratia*, *Achromobacter*, *Bacillus* and *Stenotrophomonas* on *Fusarium oxysporum* caused fungal damage through the mechanism of releasing thermolysin exoproteases and siderophores compounds (Minerdi et al., 2008). *P. aeruginosa* forms a biofilm on the surface of pseudohyphae, causing death in *Candida albicans* by releasing quorum-sensing compounds (Hogan et al., 2004, 2007). Furthermore, colonies of *Pseudomonas chlororaphis* on the hyphae surface cause the inhibition of *F. oxysporum* hyphae growth and branching *via* pyocyanin antifungal compound mechanisms (Bolwerk et al., 2003).

The current study found that *R. microsporus* was damaged during incubation time, perhaps by its interaction with the associated bacteria. The bacterium *P. aeruginosa* N1 was isolated as an associated bacterium in the hyphae of *R. microsporus*, which was suspected of having potential as a biocontrol agent. The current study aimed to determine the effect of *P. aeruginosa* N1 on the morphology of *R. microsporus*. Furthermore, the mechanism was studied of inhibition through antagonistic interactions in multiple cultures. The compounds secreted during the interaction were analyzed using Liquid Chromatography-Mass Spectrometry/Mass Spectrometry Quadrupole Time-of-Flight (LC-MS/MS Q-TOF).

Materials and Methods

Isolation and identification of R. microsporus

Initially, *R. microsporus* was isolated from a *Moringa oleifera* leaf. The *Moringa* leaf was cut and broken with sterile equipment and placed on potato dextrose agar (PDA) medium and then, the samples were incubated at room temperature for 5 d. The fungal colonies were purified by transferring to a new medium. The fact that the *Rhizopus* isolates were damaged in a few weeks during this study suggested that it interacted with another microbe with antagonistic ability against fungi. Therefore, the modified ring method (Raper, 1937) and the simple method (Cother and Priest, 2009) were applied to purify *Rhizopus*.

Isolation and identification of associated bacteria causing damage in R. microsporus

According to Minerdi et al. (2008), bacteria that caused fungal damage were isolated by incubating some damaged hyphae in a trypticase soy broth (TSB) medium to grow some associated bacteria involved in the interaction, with some modifications. The TSB medium was incubated overnight at 30 °C. The turbidity of the medium indicated bacterial growth. To obtain a pure colony, one loop of the medium was transferred to nutrient agar (NA) medium using the quadrant-streak technique and then incubated for 24 h at

30 °C. In total, 16 isolates were obtained, but only 9 of them had inhibition zones. In the chrome azurol S (CAS) agar test, the isolate *P. aeruginosa* N1 had the largest zone (data not shown). Identification of *P. aeruginosa* N1 was performed based on a molecular technique using 27F and 1492R primers (Virgianti et al., 2020). The genomic DNA was extracted using the Quick-DNATM Fungal/Bacterial Miniprep Kit (Zymo Research; D6005), and polymerase chain reaction (PCR) was performed using a Thermocycler Agilent SureCycler 8800. The DNA was purified using a Zymoclean Gel DNA Recovery Kit (Zymo Research). The sequencing was done by Genetika Science Indonesia. BLAST (http://www.ncbi.nlm.nih.gov/BLAST) was used to analyze the assembled sequence data.

Phylogenetic analysis

The neighbor-joining tree was constructed to refer phylogenetic relationship among bacterial isolates using the MEGA7 software (Kumar et al., 2016) with 1,000 bootstrapping. The evolutionary distance was computed using the maximum composite likelihood method.

Inhibition zone in dual culture assay and morphological alteration assay

Antagonism activity against *Rhizopus* was conducted using a dual culture assay, according to Zohara et al. (2016). Five-day old purified *Rhizopus* culture was cut approximately 6 mm in diameter, placed in new PDA medium and set 3 cm apart from the bacterial colony streak on the agar plate. The medium was incubated for 5 d at room temperature. The inhibition zone was characterized by the presence of a clear area around the colony. The morphological alteration of the *Rhizopus* hyphae was investigated based on microscopic morphological observations, according to Zohara et al. (2016) with slight modification. A small number of hyphae were cut from the inhibition zone and placed on a glass slide to be examined under a light microscope (Olympus CX23; 100× and 400× magnification). At least five replicated samples were analyzed, with one of them being selected to be photographed.

Detection of siderophore production of bacteria

The siderophore activity of the bacterial isolate was determined using modified CAS agar by referring to Hu and Xu (2011). CAS (60.5 mg) was dissolved in 50 mL of water and mixed with 10 mL of iron (III) solution (1 mmol/L FeCl3.6H20, 10 mmol/L HCl). Blue- indicator dye CAS solution was slowly added with constant stirring to 72.9 mg hexadecyltrimethylammonium (HDTMA), dissolved in 40 mL of water, and then autoclaved. CAS-blue agar (dye solution 10 mL) was prepared as the bottom layer agar in a Petri dish plate (9 cm in diameter). After solidifying, the Luria Bertani (LB) agar (6 mL) was poured into the CAS as a top layer. A bacteria isolate was inoculated and incubated for 5 d at 30 °C. The appearance of a yellowish-orange halo was considered to confirm bacterial siderophore production.

Scanning electron microscopy

Control hyphae and co-culture hyphae were immersed in cacodylate buffer for 2 h before being agitated in an ultrasonic cleaner for 5 min. The sample was prefixed in 2.5% glutaraldehyde for 3 h and then fixed in 2% tannic acid for 6 h. Following this, the sample was washed four times with cacodylate buffer, for a duration of 5 min each time. Then, the sample was dehydrated by immersing it in a serial alcohol graded 50%, 70%, 85% and 95% for durations of 20 min each time, and then immersing it twice in absolute alcohol for 10 min. Next, the sample was then soaked twice in tert butanol for 10 min, frozen in a freezer, and consequently dried in a freeze-dryer during the drying stages. Finally, the sample was glued to the specimen stub and coated with gold. Observations were made using scanning electron microscopy (SEM; JSM-IT200 (JEOL;InTouchScope™) at 10 kV (1000×, 3000×, 3500× and 10000×), according to Goldstein et al. (1992).

Bacterial metabolite extractions and screening of active natural material using liquid chromatography-mass spectrometry/mass spectrometry quadrupole time-of-flight

Three types of culture were grown on PDA to extract bacterial metabolites: a single culture of bacteria, a single culture of fungi and a co-culture of bacteria and fungi. In co-culture, the fungus was inoculated by transferring a single loop of hypha to 3 cm away from the bacterial streak. All three cultures were incubated for 5 d at room temperature. The metabolite extraction process was conducted with reference to Bohni et al. (2016) and Phelan et al. (2015), with modifications. Metabolite extraction was accomplished by grinding all parts of the agar in a mortar for each culture. Then, the results were macerated in ethyl acetate until completely submerged, stirred and the soaking solution was changed every 24 h, up to three times. In total 20 Petri dishes produced

approximately 1 g of crude extract. Next, the macerated solution was evaporated at 45 °*C using a rotary evaporator until a crude extract was obtained*, which was diluted using methanol. The bacterial crude extract (0.5 g) was dissolved in acetonitrile, homogenized and then passed through a 0.22 µm membrane filter unit. In total, 5 µL of sample filtrate was injected into the Ultra Performance LC (UPLC) in an ACQUITY UPLC® I-Class System. The MS system used was Xevo® G2 QTof MS. The mode of operation was Tof MS^{E}. LC-MS/MS analysis was equipped with a binary pump, and the LC connected Q-TOF mass spectrometer was equipped with an electrospray ionization (ESI) source. The acquisition range was 50–1200 Da, the scan time was 0.1 s, the capillary voltage was 3 KV (ESI +)/2.5 KV (ESI -), the cone voltage was 100 V, the source temperature was 120 °*C,* the desolvation temperature was 500 °*C,* the cone gas flow was 30 L/h, the desolvation gas flow was 1,000 L/h and the acquisition time was 20 min. The LC column used by in the Acquity UPLC HSS C18 equipment was 1.8 µm (2.1 mm ×150 mm). The effluents used were 0.1% formic acid in acetonitrile p.a. (A) and 0.1% formic acid in H_2O (B). The column temperature was 40 °*C* and the Autosampler temperature was 15°C. The injection volume was 10 µL. The effluent was set at a total flow rate of 0.6 mL/min. The interpretation of LC-MS/MS was made in reference to the mass spectrum Waters database library using the UNIFI system. The active substance was identified under the following conditions: mass error of analyte reading ≤ 5 parts per million error; isotope match *MZ RMS* ≤ 6; and analyte intensity ≥300; There was one fraction with brake value < 4 in the Fragment Match elucidation system (Qiao et al., 2013).

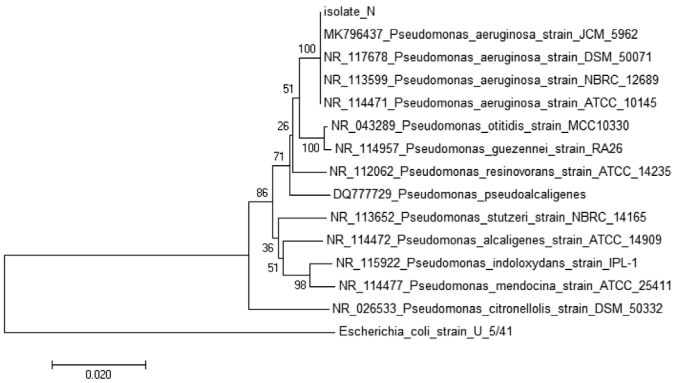

Fig. 1 Neighbor-joining phylogenetic dendrogram based on 16S rRNA sequences showing phylogenetic relationships between bacterial *Pseudomonas aeruginosa* isolate N1 and closely related strains to *P. aeruginosa*, with bootstrap values based on 1,000 replicates shown at branch nodes and tree places bacterial isolates into *P. aeruginosa* clade

Results

Isolation and identification of bacterial strains.

Damage to *R. microsporus* hyphae is considered a manifestation of its interaction with bacteria. Based on the results of bacterial isolation obtained from the damaged hyphae of *R. microsporus*, Gram-negative rods were obtained. Bacterial colonies were creamy-white, non-pigmented, semi-translucent, circular, medium in diameter, raised in elevation, with undulated margins and slightly shiny. In cultured medium, it produced a yellow-orange pigment. The bacterial isolate was identified as *P. aeruginosa* N1. The 16S rRNA sequence of isolate N1 was successfully amplified. The PCR product showed a DNA fragment with a length of 1500 bp. The BLAST results of the 16 rRNA sequences (1,408 nucleotides) showed similarities to *P. aeruginosa* (99.93%). These results were in agreement with the phylogenetic tree analyzed using NJ, which showed that the closest family was in the same clade with *P. aeruginosa* (Fig. 1).

Antagonistic activity of associated bacteria on R. microsporus

According to the dual culture assay, *P. aeruginosa* N1 inhibited the growth of *R. microsporus*, as evidenced by the resulting inhibition zone compared to the control (Fig. 2). Based on the observations of hyphae in the zone of inhibition, changes were observed compared to the control, namely the presence of hyphae with curly and wrinkled shapes and reduced spore formation at the tips of the hyphae (Fig. 3). Observation of hyphal damage was continued based on SEM examination.

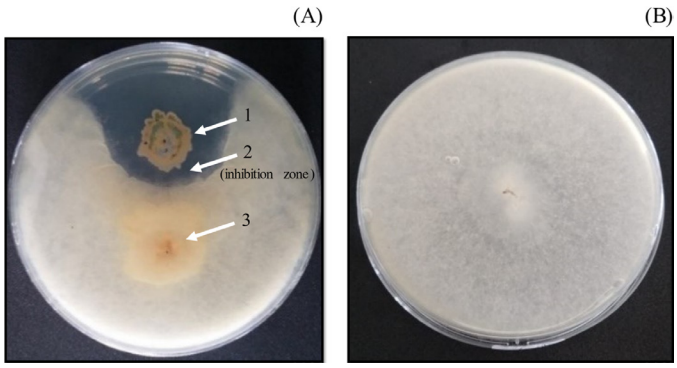

Fig. 2 (A) Dual culture assay between *Pseudomonas aeruginosa* N1 (1) and *Rhizopus microsporus* (3) showing a zone of inhibition around the bacterial colonies (2); (B) fungal control

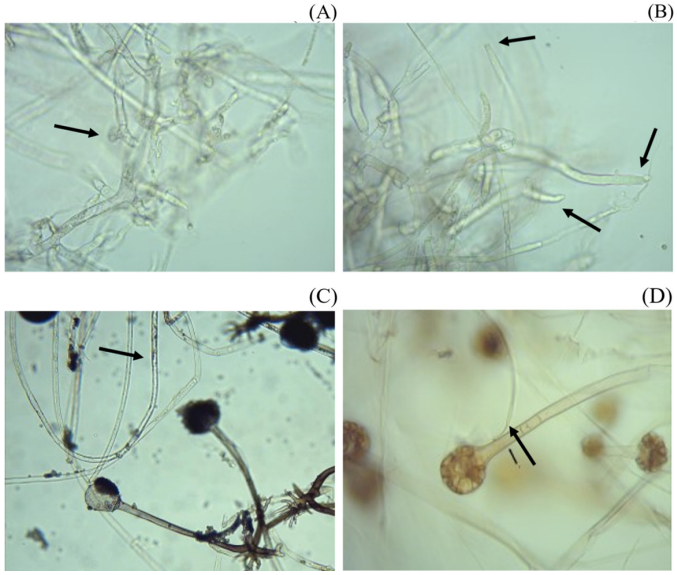

Fig. 3 Hyphae taken from inhibition zone showing change in shape to curly hyphae (A); and no spore formation at the ends of hyphae (B); compared to hyphae in control showing normal, straight hyphae (C); and spore formation (D)

The results showed that there appeared to be differences in the hyphal morphology of the control hyphae compared to that of co-culture hyphae. The control hyphae were straight and had a smooth surface, while the co-culture hyphae were wrinkled and had a wrinkled surface (Fig. 4). In addition, the wrinkled hyphae showed *P. aeruginosa* N1 bacteria that accumulated on the surface of the damaged hyphae. These bacteria may have colonized and formed biofilms on the hyphal surface and released their metabolites, thereby causing damage.

Production of active compounds by P. aeruginosa N1.

The production of iron-chelating compounds in *P. aeruginosa* N1 was tested on CAS agar media containing iron Fe3+ bound to HDTMA compounds. The bacterial growth resulted in yellow pigment formation that tended to grow larger (Fig. 5). This condition indicated that the isolate produced compounds that could bind iron, allowing iron to be released from the binding compound in the medium, indicated by the color turning yellow-orange when untied.

Analysis using LC-MS/MS was performed on the compounds in the *P. aeruginosa* N1 monoculture, the *R. microsporus* monoculture and the *P. aeruginosa* N1 co-culture with *R. microsporus* grown in one Petri dish to confirm the active compound released by *P. aeruginosa* N1 in inhibiting the growth of *R. microsporus*. The target compounds examined were active in *Pseudomonas* bacteria, namely phenazine, pyoverdine, pyocyanin, pyoluteorine, homoserine lactone (HSL) compounds, pseudomonas quinolone signal (PQS) and rhamnolipid compounds. The LC-MS/MS analysis revealed the presence of active compounds, such as phenazine group compounds, PQS and rhamnolipids (Table 1).

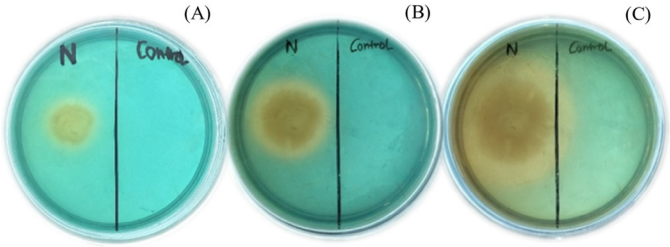

Fig. 5 Formation of yellow zone on CAS agar indicating isolate *P. aeruginosa* N1 produces compounds that can hold iron, with yellow zone formation expanding following incubation for: (A) 1 day; (B) 3 days; (C) 5 days

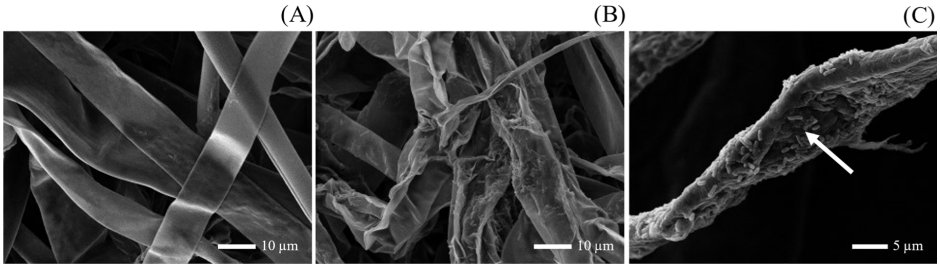

Fig. 4 Scanning electron micrograph showing control fungi with intact hyphae and smooth surface (A); while hyphae from inhibition zones show damage as wrinkles on hyphal surface (B), where arrow indicates biofilm of *P. aeruginosa* N1 on hyphal surface (3,000× magnification) in (C)

Table 1 Recapitulation of confirmed components of *Pseudomonas aeruginosa* N1 active compound in monocultures and co-cultures examined using liquid chromatography-mass spectrometry/mass spectrometry quadrupole time-of-flight showing differences in appearances of several compounds

No	ESI mode	Compound name	m/z	Result		
				Pseu	Rhiz	Co-culture
1	Pos	1-Hydroxyphenazine (1-HP)	197.0707	+	-	+
2	Pos	1-Phenazinecarboxylic acid (PCA)	225.0664	+	-	+
3	Pos/ Neg	2-Nonyl-4-hydroxyquinoline N-OXIDE (NQNO)	286.1810	+	-	-
4	Pos/ Neg	2-Heptyl-hydroxy-4(1H)-quinolone (PQS)	260.1639	+	-	+
5	Pos	2-Nonyl-4-quinolinone (NHQ)	272.2001	+	-	+
6	Pos/ Neg	2-Undecyl-4(1H)-quinolone (UHQ)	300.2316	+	-	+
7	Neg	2-Heptyl-4-hydroxyquinoline n-oxide (HQNO)	258.1500	+	-	+
8	Pos	2-Heptyl-4-quinolone (HHQ)	244.1691	-	-	+
9	Pos	1-Hydroxy-2-[(2E)-2-nonen-1-yl]-4(1H)-quinolinone	286.1795	-	-	+
10	Neg	2-Nonyl-3-hydroxy-4-quinolone (C9- PQS)	286.1813	-	-	+
11	Neg	mono-rhamnolipid	503.3231	+	-	-
12	Neg	di-Rhamnolipid	649.3812	+	-	+

Pos = Positive; Neg = negative; + = detected; - = not detected; Pse = *Pseudomonas*; Rhi = *Rhizopus*; ESI = electrospray ionization

Discussion

The *P. aeruginosa* N1 isolate shared characteristics with other *P. aeruginosa* isolated from the environment, such as the M18 isolate reported by Hu et al. (2005). The *Pseudomonas* genus, which produces phenazine, is frequently used as a biocontrol agent strain, including *P. fluorescence* (Thomashow and Weller, 1988) and *P. chlororaphis* (Chin-A-Woeng et al., 2000).

Phenazine is a naturally occurring heterocyclic redox-active compound in the form of a reduced solution. The aromatic rings are substituted by different functional groups, resulting in various derived colors. The natural colors of the four different phenazines that *P. aeruginosa* species can produce are yellow for phenazine carboxamide (PCN) and PCA, orange for 1-hydroxyphenazine (1-HP) and blue for pyocyanin. The pigment made by *P. aeruginosa* isolate N1 was yellow-orange, indicating that the phenazines produced were PCA and 1-HP. This condition was confirmed by the compound analysis data detected using LC-MS/MS, specifically PCA and 1-HP in both cultures, namely the *P. aeruginosa* N1 monoculture and the *P. aeruginosa* N1 co-culture with *R. microsporus* (Table 1). The mechanism of inhibition of *R. microsporus* growth in co-culture with *P. aeruginosa* N1 is primarily due to phenazine compounds, while PCA is considered the main biocontrol compound as an antifungal (Mavrodi et al., 2006).

PCA can reduce Fe (III) to Fe (II), which bacteria take up via ferrous iron transporters (Hernandez et al., 2004). PCA is antifungal at high concentrations because it can penetrate cells and induce the production of reactive oxygen species and reactive nitrogen species, particularly in mitochondria, causing mitochondrial changes and fungal cell death (Briard et al., 2015). In addition to PCA, *P. aeruginosa* N1 produced other phenazine derivative compounds, such as 1-HP, which has antifungal properties. Among other phenazines, the mechanism of inhibition of 1-HP against fungi is the most active (Briard et al., 2015. 1-HP is an iron chelator that can bind to Fe (III) in the environment, causing fungal growth to be inhibited in iron-deficient environments (Briard et al., 2015). The ability of phenazine to chelate iron was indicated by yellow zone formation around the colony on the CAS agar (Fig. 5). In the presence of phenazines, which modify the morphology of hyphae and mitochondria, swelling and germination were delayed significantly in *Aspergillus fumigatus* and *Phytophthora capsici* (Briard et al., 2015; Zohara et al., 2016). This condition also occurred in *Rhizopus* in the present study, in which the *P. aeruginosa* N1 isolate inhibited fungal germination and altered the hyphal morphology, causing the hyphae to appear curly (Fig. 3) with wrinkles on the surface (Fig. 4).

The present study revealed a different regulation in the strains identified, namely the role of the PQS as a quorum-sensing molecule in the production of phenazine that occurred. Quorum sensing (QS) is *P. aeruginosa*'s main virulence strategy, which serves as cell-cell communication and ultimately leads to the production of several virulence factors (Williams and Camara, 2009). *P. aeruginosa* has a sophisticated QS network consisting of four different-but-interconnected systems, namely LasI/LasR, Rrhl/RhIR, PQS/MvfR and IQS, and their cognate QS signaling molecules (QSMs). The essential QSMs in *Pseudomonas* are acyl homoserine lactones and AQs (Chatterjee et al., 2020). The QS system's mechanism for controlling the expression of phenazine-producing genes differs between strains. In the clinical isolates *P. aeruginosa* PA01 and

PA14, phenazine compound production was regulated in a hierarchical cascade via the Las-and Rhl-system (Price-Whelan et al., 2006). The Las and Rhl systems appear to be negative regulators of phenazine production in *P. aeruginosa* M18 isolated from the rhizosphere. It is regulated by direct RNA-binding protein RmsA's-mediated, activating *phz*2 expression (Ren et al., 2014). In another rhizosphere-isolated strain, *P. aeruginosa* P1201, both the C4-HSL/RhiR and PQS/MvfR systems positively up regulated the expression of *phz*1 and *phz*2 to promote PCA production (Sun et al., 2016).

In the *P. aeruginosa* N1 sample in the present study, the detected QSMs were only AQs (Table 1). The role of AQs in regulating phenazine production lies in its ability to bind to its receptor, namely MvfR in the *phz*A1-G2 and *phz*A2-G2 gene clusters. MvfR is one of the most important QS regulators in *P. aeruginosa* (Wade et al., 2005). The PQS signal receptor MvfR regulates 2-heptyl-4-quinolone (HHQ) and PQS biosynthesis by binding the promoter of pqsABCDE (Wade et al., 2005; Fang et al., 2018). MvfR is essential for PCA biosynthesis in strain *P. aeruginosa* PA1201 (Sun et al., 2016). Complexity to the QS regulation of PCA biosynthesis in *P. aeruginosa* differs between the strains. However, both *phz* clusters contributed significantly to PCA production, with *phz*2 contributing the most in *P. aeruginosa* strains P1201, M18 and PA14 (Recinos et al., 2012; Sun et al., 2016). In *phz*2, PCA production is a quinolone-dependent regulation, but quinolone removal also abolished PCA production in *phz*1. This suggested that PQS and its precursor HHQ positively regulate phenazine production from *phz*2 (Recinos et al., 2012). While *phz1* is more involved in pyocyanin production, the positions of the operons on the chromosome of *P. aeruginosa* PAO1 showed that the *phz1* operon was clustered with the genes required to produce pyocianine; thus, it may be more closely associated with pyocyanin production than *phz2* (Higgins et al., 2018).

In the monoculture of *P. aeruginosa* N1 and the co-culture with *R. microsporus*, PCA and 1-HP were produced, but there were differences in the AQs signal produced (Table 1). Quinolones are extremely diverse, with acyl chain lengths in the range 3–17 carbons in the three *Pseudomonas* quinolone signal base forms of PQS, HHQ and 2-heptyl-4-quinolone-N-oxide (HQNO), according to Lybbert et al. (2020). A study used electrospray ionization and LC-MS to obtain the mass spectra of over 50 different AQs (Fletcher et al., 2010).

PQS was discovered in both cultures in the present study (Table 1). PQS acts as an iron chelating compound (Lin et al., 2018) in addition to being a regulator of the *phz* gene, which produces PCA (Recinos et al., 2012). PQS has a high affinity for the ferrous iron (Fe^{3+}) and reduces the availability of free iron in the environment by binding to iron (Diggle et al., 2007; Lin et al., 2018). Thus, PQS can act as an iron trap and storage molecule in cell membranes and transport iron to bacterial cells (Lin et al., 2018).

C9-PQS and HHQ were only detected in co-cultures between *P. aeruginosa* N1 and *R. microsporus* and not in the bacterial monoculture (Table 1). In addition to PQS (7 carbon side chains), *P. aeruginosa* naturally produced PQS analogues with alkyl side chain lengths of 5 and 9 molecules (Schertzer et al., 2010). Compared to another alkyl PQS, C9-PQS was almost as strong as PQS in inhibiting fungal (*A. flavus*) growth on agar (Nazik et al., 2021). C9-PQS and HHQ can also bind Fe^{3+} (Diggle et al., 2007; Fletcher et al., 2010; Lin et al., 2018). HHQ is a diffusible messenger molecule produced in cells and then converted into PQS by the flavin-dependent monooxygenase encoded by the pqsH gene, which is located far from the PQS operon (Deziel et al., 2004; Schertzer et al., 2010). Both HHQ and PQS possess the ability to alter the morphology, biofilm, biomass and hyphal structure of fungi such as *A. fumigatus* (Reen et al., 2016). PQS was found in the monoculture of *P. aeruginosa* N1 in the present study, but not HHQ (Table 1), indicating that the precursor (HHQ) had been completely converted to PQS. HHQ is produced in the middle of the log phase (Deziel et al., 2004; Buzid et al., 2016) and the number of HHQs begins to decrease while the number of PQSs increases in the stationary phase (Buzid et al., 2016). HHQ should be converted to PQS in the co-cultures used in the present study. Cao et al. (2020) demonstrated that under stress conditions, such as when there are competitors or limited carbon sources, PQS is produced earlier. However, HHQ was still detected in the co-culture on the fifth day of growth (Table 1) suggesting that HHQ plays a role in pathogenicity against competing microorganisms. In clinical cases, *P. aeruginosa* caused cystic fibrosis and on day 11, HHQ was more dominant than PQS in sputum samples (Buzid et al., 2016). In addition, HHQ acts as a modulator in the movement of *P. aeruginosa* bacteria, which can repress swarming motility that causes stimulation of biofilm formation (Ha et al., 2011).

The culture also contained AQNOs, a 2-alkyl-4-hydroxyquinoline N-oxide derivate of AQs (Table 1). The most common examples are heptyl and nonyl-substituted derivatives, but 8- and 11-carbon analogues, as well as a small suite of unsaturated derivatives, have also been reported (Saalim et al., 2020). The AQNOs possess considerable antibacterial activity. Mashburn and Whiteley (2005) showed

that membrane vesicles derived from *P. aeruginosa* culture contained PQS and HQNO, which displayed antimicrobial activity to protect the *P. aeruginosa* niche from competitors. Cao et al. (2020) revealed that HQNO and PQS were produced in monocultures or co-cultures with other microbes, but their production was faster in co-cultures in response to stress in the presence of competitors. In addition, there are differences in the distribution of HQNO and PQS, where HQNO is spread far from the *P. aeruginosa* growth area to the competitor microbial area, whereas PQS is not far removed (Cao et al., 2020).

Rhamnolipids were found in the monoculture and co-culture (Table 1). Mono-rhamnolipid was found in the monoculture, while rhamnolipid was found in the co-culture. Lybbert et al. (2020) demonstrated that rhamnolipids were restricted to one or two sugars with a limited set of fatty acyl chains. Rhamnolipids are produced by *P. aeruginosa* and act as biosurfactants. They facilitate swarming motility (Caiazza et al., 2005) and the detachment of cells from *P. aeruginosa* biofilm (Boles et al., 2005). Another study showed that *P. aeruginosa* rhamnolipids acted as an antifungal on a range of fungal species, including *Candida albicans*, *F. oxysporum* and *A. fumigatus* (Gibson et al., 2009; Briard et al., 2017). Di-rhamnolipid binds to fungal hyphae through the extracellular matrix (ECM) polysaccharide galactosaminogalactan (GAG) and induces GAG and melanin production in the ECM (Briard et al., 2017). Simultaneously, di-rhamnolipids increase chitin synthesis, compensating for inhibiting 1,3-beta-glucan synthase, promoting new apices (Briard et al., 2017; Briard et al., 2019). This mechanism interaction results in hyphal wall thickening and altered development of fungal hyphae with short ramifications at the tip (Briard et al., 2017; Briard et al., 2019). In addition, rhamnolipid acts as a biodetergent by increasing the solubility and bioactivity of PQS (Calfee et al., 2005). The presence of di-rhamnolipid in the co-culture of *P. aeruginosa* N1 and *R. microsporus* (Table 1) was due to a response in *P. aeruginosa* pathogenicity against *R. microsporus*. Only rhamnolipids were detected in the monoculture because no further synthesis was required to form di-rhamnolipid. The effect of the presence of di-rhamnolipid on *R. microsporus* was seen in the form of changes in the hyphal structure, namely the modification of the hyphal phenotype to curly and irregular. This may have been due to GAG induction in the hyphal ECM of *P. aeruginosa* N1 (Fig. 4). As stated before, rhamnolipid acts as a biodetergent by increasing the solubility and bioactivity of PQS; this increased solubility correlates with the ability of PQS to induce lasB exposure (Calfee et al., 2005). LasB encodes the production of lasB elastase, which, in turn, plays a role in helping bacterial attachment, micro colony formation and extracellular matrix linkage in biofilms (Yu et al., 2014). This protease produced by *P. aeruginosa* was notably higher in the presence of fungus in the co-culture experiments (Smith et al., 2015).

The production of pyoverdine compounds by *P. aeruginosa* N1 was not detected. This was consistent with *P. aeruginosa* M18, which was found to lack the gene encoding the pyoverdine Pvds gene (PALES28681) in its whole genome (Wu et al., 2011). This suggested that the iron-chelating compounds detected in the CAS agar test (Fig. 5) were the quinolones, PQS, C9-PQS, and HHQ rather than pyoverdine.

The present study highlighted the complexity of QS regulation and that active compound biosynthesis in *P. aeruginosa* differs between species. Additionally, the interaction mechanism between *P. aeruginosa* N1 isolate and *R. microsporus* has been examined, where the compounds detected by LC-MS/MS were critical. The complexity of the interactions should be studied further, especially to increase the production of active compounds so that *P. aeruginosa* N1 isolates can be used as a biocontrol against harmful microbes, particularly in the agricultural sector.

Conflict of Interest

The authors declare that there are no conflicts of interest.

Acknowledgements

This research was funded by a Budi-DN LPDP Indonesia Scholarship.

References

Bohni, N., Hofstetter, V., Gindro, K., Butck, B., Schumpp, O., Bertrand, S., Monod, M., Wolfender, J-L. 2016. Production of fusaric acid by *Fusarium* spp. in pure culture and in solid medium co-cultures. Molecules 21: 370. doi.org/10.3390/molecules21030370

Boles, B.R., Thoendel, M., Singh, P.K. 2005. Rhamnolipids mediate detachment of *Pseudomonas aeruginosa* from biofilms. Mol. Microbiol. 57: 1210–1223. doi.org/10.1111/j.1365-2958.2005.04743.x

Bolwerk, A., Lagopodi, A.L., Wijfjes, A.H.M., Lamers, G.E.M., Chin-A-Woeng, T.F.C., Lugtenberg, B.J.J., Bloemberg, G.V. 2003. Interactions in the tomato rhizosphere of two *Pseudomonas* biocontrol strains with the phytopathogenic fungus *Fusarium oxysporum* f. sp. radicis-lycopersici. Mol. Plant Microbe Interact. 16: 983–999. doi.org/10.1094/MPMI.2003.16.11.983

Briard, B., Bomme, P., Lechner, B.E., et al. 2015. *Pseudomonas aeruginosa* manipulates redox and iron homeostasis of its microbiota partner *Aspergillus fumigatus* via phenazines. Sci. Rep. 5: 8220. doi.org/10.1038/srep08220

Briard, B., Mislin, G.L.A., Latgé, J.P., Beauvais, A. 2019. Interactions between *Aspergillus fumigatus* and pulmonary bacteria: Current state of the field, new data, and future perspective. J. Fungi Basel. 5: 48. doi.org/10.3390/jof5020048

Briard, B., Rasoldier, V., Bomme, P., et al. 2017. Dirhamnolipids secreted from *Pseudomonas aeruginosa* modify antifungal susceptibility of *Aspergillus fumigatus* by inhibiting β1,3 glucan synthase activity. ISME J. 11: 1578–1591. doi.org/10.1038/ismej.2017.32

Buzid, A., Shang, F., Reen, F.J., et al. 2016. Molecular signature of *Pseudomonas aeruginosa* with simultaneous nanomolar detection of quorum sensing signaling molecules at a Boron-doped diamond electrode. Sci. Rep. 6: 30001. doi.org/10.1038/srep30001

Caiazza, N.C., Shanks, R.M., O'Toole, G.A. 2005. Rhamnolipids modulate swarming motility patterns of *Pseudomonas aeruginosa*. J. Bacteriol. 187: 7351–7361. doi.org/10.1128/JB.187.21.7351-7361.2005

Calfee, M.W., Shelton, J.G., McCubrey, J.A., Pesci, E.C. 2005. Solubility and bioactivity of the *Pseudomonas* quinolone signal are increased by a *Pseudomonas aeruginosa*-produced surfactant. Infect. Immun. 73: 878–882. doi.org/10.1128/IAI.73.2.878-882.2005

Cao, T., Sweedler, J.V., Bohn, P.W., Shrout, J.D. 2020. Spatiotemporal distribution of *Pseudomonas aeruginosa* alkyl quinolones under metabolic and competitive stress. mSphere 5: e00426-20. doi.org/10.1128/mSphere.00426-20

Chatterjee, P., Sass, G., Swietnicki, W., Stevens, D.A. 2020. Review of potential *Pseudomonas* weaponry, relevant to the *Pseudomonas-Aspergillus* interplay, for the Mycology Community. J. Fungi. Basel 6: 81. doi.org/10.3390/jof6020081

Chin-A-Woeng, T.F.C., Bloemberg, G.V., Mulders, I.H.M, Dekkers, L.C., Lugtenberg, B.J.J. 2000. Root colonization by phenazine-1-carboxam- ide-producing bacterium *Pseudomonas chlororaphis* PCL1391 is essential for biocontrol of tomato foot and root rot. Mol. Plant Microbe Interact. 13: 1340–1345. /doi.org/10.1094/MPMI.2000.13.12.1340

Cother, N.J., Priest, M. J. 2009. A simple and effective method for the elimination of bacteria from fungal cultures. Australas. Plant Path. 38: 132–134. doi.org/10.1071/AP08096

Deziel, E., Lepine, F., Milot, S., He, J., Mindrinos, M.N., Tompkins, R.G., Rahme, L.G. 2004. Analysis of *Pseudomonas aeruginosa* 4-hydroxy-2- alkylquinolines (HAQs) reveals a role for 4-hydroxy-2-heptylquinoline in cell-to-cell communication. Proc. Natl. Acad. Sci. U S A 101: 1339–1344. doi.org/10.1073/pnas.0307694100

Diggle, S.P., Matthijs, S., Wright, V.J., et al. 2007. The *Pseudomonas aeruginosa* 4-quinolone signal molecules HHQ and PQS play multifunctional roles in quorum sensing and iron entrapment. Chem. Biol. 14: 87–96. doi.org/10.1016/j.chembiol.2006.11.014

Dolatabadi, S., Olecka, A., Versteeg, M., de Hoog, G.S., Boekhout, T. 2015. Differentiation of clinically relevant mucorales *Rhizopus microsporus* and *R. Arrhizus* by matrix-assisted laser desorption ionization time-of-flight mass spectrometry (MALDI-TOF MS). J. Med. Microbiol. 64: 694–701. doi.org/10.1099/jmm.0.000091

Fang, Y.L., Chen, B., Zhou, L., Jin, Z.J., Sun, S., He, Y.W. 2018. The anti-activator QslA negatively regulates Phenazine-1-Carboxylic acid biosynthesis by interacting with the quorum sensing regulator MvfR in the rhizobacterium *Pseudomonas aeruginosa* strain PA1201. Front. Microbiol. 9: 1584. doi.org/10.3389/fmicb.2018.01584

Fletcher, M.P., Heeb, S., Chhabra, S.R., Diggle, S.P., Williams, P., Cámara, M. 2010. Psedomonas. In: Ramos, J.L., Filloux, A. (Eds.). 2-Alkyl-4(1*H*)-Quinolone Signalling in *Pseudomonas aeruginosa*. Springer. London, UK, pp. 29–57. doi.org/10.1007/978-90-481-3909-5_2

Frey-Klett, P., Burlinson, P., Deveau, A., Burret, M., Tarkka, M., Sarniguet, A. 2011. Bacterial-fungal interaction: Hyphens between agricultural, clinical, environmental, and food microbiologists. Microbiol. Mol. Biol. Rev. 75: 583–609. doi.org/10.1128/MMBR.00020-11

Gibson, J., Sood, A., Hogan, D.A. 2009. *Pseudomonas aeruginosa-Candida albicans* interactions: Localization and fungal toxicity of a phenazine derivative. Appl. Environ. Microbiol. 75: 504–513. doi.org/10.1128/AEM.01037-08

Goldstein, J.I., Newbury, D.E., Echlin, P., Joy, D.C., Romig, A.D., Lyman, Jr., C. E.,Fiori, C., Lifshin, E. 1992. Scanning Electron Microscopy and X-ray Microanalysis: A Text for Microbiologist, Material Scientist, and Cytologists, 2nd ed. Plemun Press. New York, NY, USA.

Ha, D.G., Merritt, J.H., Hampton, T.H., et al. 2011. 2-Heptyl-4-Quinolone, a precursor of the *Pseudomonas* quinolone signal molecule, modulates swarming motility in *Pseudomonas aeruginosa*. J. Bacteriol. 193: 6770–6780.

Hernandez, M.E., Kappler, A., Newman, D.K. 2004. Phenazines and other redox-active antibiotics promote microbial mineral reduction. Appl. Environ. Microbiol. 70: 921–928. doi.org/10.1128/AEM.70.2.921-928.2004

Higgins, S., Heeb, S., Rampioni, G., Fletcher, M.P., Williams, P., Cámara, M. 2018. Differential regulation of the phenazine biosynthetic operons by quorum sensing in *Pseudomonas aeruginosa* PAO1-N. Front. Cell. Infect. Microbiol. 8: 252. doi.org/10.3389/fcimb.2018.00252

Hogan, D., Vik, A., Kolter, R. 2004. A *Pseudomonas aeruginosa* quorum-sensing molecule influences *Candida albicans* morphology. Mol. Microbiol. 54: 1212–1223. doi.org/10.1111/j.1365-2958.2004.04349.x

Hogan, D.A., Wargo, M.J., Beck, N. 2007. Bacterial biofilm on fungal surfaces. In: Kjelleberg, S., Givskov, M. (Eds.). The Biofilm Mode of Life: Mechanisms and Adaptations. Horizon Scientific Press. Poole, UK, pp. 235–245.

Hong, J., White, J.D. 2004. The chemistry and biology of rhizoxins, novel antitumor macrolides from *Rhizopus chinensis*. Tetrahedron 60: 5653–5681. doi.org/10.1016/j.tet.2004.04.032

Hu, H.B., Xu, Y.Q., Chen, F., Zhang, X.H., Hur, B.K. 2005. Isolation and characterization of a new fluorescent *Pseudomonas* strain that produces both phenazine 1-Carboxylic acid and pyoluteorin. J. Microbiol. Biotechnol. 15: 86–90.

Hu, Q.P., Xu, J.G. 2011. A simple double-layered chrome azurol S agar (SD-CASA) plate assay to optimize the production of siderophores by a potential biocontrol agent *Bacillus*. Afr. J. Microbiol. Res. 5: 4321–4327. doi: 10.5897/AJMR11.238

Jennessen, J., Nielsen, K.F., Houbraken, J., Lyhne, E.K., Schnurer, J., Frisvad, J.C., Samson, R.A. 2005. Secondary metabolite and mycotoxin production by the *Rhizopus microsporus* group. J. Agric. Food Chem. 53: 1833–1840. doi.org/10.1021/jf048147n

Kousser, C., Clark, C., Sherrington, S., Voelz, K., Hall, R.A. 2019. *Pseudomonas aeruginosa* inhibits *Rhizopus microsporus* germination through sequestration of free environmental iron. Sci. Rep. 9: 5714. doi.org/10.1038/s41598-019-42175-0

Kumar, S., Stecher, G., Tamura, K. 2016. MEGA7: Molecular evolutionary genetics analysis version 7.0 for bigger datasets. Mol. Biol. Evol. 33: 1870–1874. doi.org/10.1093/molbev/msw054

Lin, J., Cheng, J., Wang, Y., Shen, X. 2018. The *Pseudomonas* quinolone signal (PQS): Not just for quorum sensing anymore. Front. Cell. Infect. Microbiol. 8: 230. doi.org/10.3389/fcimb.2018.00230

Lybbert, A.C., Williams, J.L., Raghuvanshi, R., Jones, A.D., Quinn, R.A. 2020. Mining public mass spectrometry data to characterize the diversity and ubiquity of *P. aeruginosa* specialized metabolites. Metabolites 10: 445. doi.org/10.3390/metabo10110445

Mashburn, L.M., Whiteley, M. 2005. Membrane vesicles traffic signals and facilitate group activities in a prokaryote. Nature 15: 422–425. doi.org/10.1038/nature03925

Mavrodi, D.V., Blankenfeldt, W., Thomashow, L.S. 2006. Phenazine compounds in fluorescent *Pseudomonas spp*.: Biosynthesis and regulation. Annu. Rev. Phytopathol. 44: 417–445. doi.org/10.1146/annurev.phyto.44.013106.145710

Minerdi, D., Moretti, M., Gilardi, G., Barberio, C., Gullino, M.L., Garibaldi, A. 2008. Bacterial ectosymbionts and virulence silencing in a *Fusarium oxysporum* strain. Environ. Microbiol. 10: 1725–1741. doi.org/10.1111/j.1462-2920.2008.01594.x

Nazik, H., Sass, G., Williams, P., Déziel, E., Stevens, D.A. 2021. Molecular modifications of the *Pseudomonas* quinolone signal in the intermicrobial competition with *Aspergillus*. J. Fungi. Basel 7: 343.

Phelan, V.V, Fang, J., Dorrestein, P.C. 2015. Mass spectrometry analysis of *Pseudomonas aeruginosa* treated with Azithromycin. J. Am. Soc. Mass Spectrom. 26: 873–877. doi.org/10.1007/s13361-015-1101-6

Pitt, J.I., Hocking, A.D. 2009. Fungi and Food spoilage, 3rd ed. Springer. New York, NY, USA.

Price-Whelan, A., Dietrich, L.E.P., Newman, D.K. 2006. Rethinking 'secondary' metabolism: Physiological roles for phenazine antibiotics. Nat. Chem. Biol. 2: 71–78. doi.org/10.1038/nchembio764

Qiao, L., Lewis, R., Hooper, A., Morphet, J., Tan, X., Yu, K. 2013. Waters application note; Using natural product application solution with UNIFI for the identification of chemicals ingredients of green tea extract. https://www.waters.com/waters/library.htm?cid=511436&lid=134775221&locale=en_US, 11 November 2022.

Raper, J.R. 1937. A method of freeing fungi from bacterial contamination. Science 85: 342. doi: 10.1126/science.85.2205.342.a

Recinos, D.A., Sekedat, M.D., Hernandez, A., Cohen, T.S., Sakhtah, H., Prince, A.S., Price-Whelan, A., Dietrich, L.E.P. 2012. Redundant phenazine operons in *Pseudomonas aeruginosa* exhibit environment-dependent expression and differential roles in pathogenicity. Proc. Natl. Acad. Sci. U. S. A. 109: 19420–19425. doi.org/10.1073/pnas.121390110

Reen, F.J., Phelan, J.P., Woods, D.F., Shanahan, R., Cano, R., Clarke, S., McGlacken, G.P., O'Gara, F. 2016. Harnessing bacterial signals for suppression of biofilm formation in the nosocomial fungal pathogen *Aspergillus fumigatus*. Front. Microbiol. 7: 2074. doi.org/10.3389/fmicb.2016.02074

Ren, B., Shen, H., Lu, Z.J., Liu, H., Xu, Y. 2014. The *phz*A2-G2 transcript exhibits direct RsmA-Mediated activation in *Pseudomonas aeruginosa* M18. PLoS One 9: e89653. doi.org/10.1371/journal.pone.0089653

Saalim, M., Villegas-Moreno, J., Clark, B.R. 2020. Bacterial alkyl-4-quinolones: Discovery, structural diversity and biological properties. Molecules 25: 5689. doi.org/10.3390/molecules25235689

Schertzer, J.W., Brown, S.A., Whiteley, M. 2010. Oxygen levels rapidly modulate *Pseudomonas aeruginosa* social behaviours via substrate limitation of PqsH. Mol. Microbiol. 77: 1527–1538. doi.org/10.1111/j.1365-2958.2010.07303.x

Smith, K., Rajendran, R., Kerr, S., Lappin, D.F., Mackay, W.G., Williams, C., Ramage, G. 2015. *Aspergillus fumigatus* enhances elastase production in *Pseudomonas aeruginosa* co-cultures. Med. Mycol. 53: 645–655. doi.org/10.1093/mmy/myv048

Sun, S., Zhou, L., Jin, K., Jiang, H., He, Y.W. 2016. Quorum sensing systems differentially regulate the production of phenazine-1-carboxylic acid in the rhizobacterium *Pseudomonas aeruginosa* PA1201. Sci. Rep. 6: 30352. /doi.org/10.1038/srep30352

Thomashow, L.S., Weller, D.M. 1988. Role of a phenazine antibiotic from *Pseudomonas fluorescens* in biological control of *Gaeumannomyces graminis* var. tritici. J. Bacteriol. 170: 3499–3508. doi.org/10.1128/jb.170.8.3499-3508.1988

Udoh, I.P., Eleazar, C.I., Ogeneh, B.O., Ohanu, M.E. 2015. Studies on fungi responsible for the spoilage/deterioration of some edible fruits and vegetables. Adv. Microbiol. 5: 285–290. doi: 10.4236/aim.2015.54027

Virgianti, D.P., Natalia, D., Aryantha, I.N.P. 2020. Short communication: New record of *Stenotrophomonas sp*. as endosymbiont bacteria in *Rhizopus microsporus*. Biodiversitas 21: 1678–1685. doi.org/10.13057/biodiv/d210449

Wade, D.S., Calfee, M.W., Rocha, E.R., Ling, E.A., Engstrom, E., Coleman, J.P., Pesci, E.C. 2005. Regulation of pseudomonas quinolone signal synthesis in *Pseudomonas aeruginosa*. J. Bacteriol. 187: 4372–4380. doi.org/10.1128/JB.187.13.4372-4380.2005

Williams, P., Camara, M. 2009. Quorum sensing and environmental adaptation in *Pseudomonas aeruginosa*: A tale of regulatory networks and multifunctional signal molecules. Curr. Opin. Microbiol. 12: 182–191. doi.org/10.1016/j.mib.2009.01.005

Wu, D.Q., Ye, J., Ou, H.Y, Wei, X., Huang, X., He, Y.W., Xu, Y. 2011. Genomic analysis and temperature-dependent transcriptome profiles of the rhizosphere originating strain *Pseudomonas aeruginosa* M18. BMC Genomics 12: 438. doi.org/10.1186/1471-2164-12-438

Xu, Y. 2013. Genomic features and regulation of phenazine biosynthesis in the rhizosphere strain *P. aeruginosa* M18. In: Chincholkar, S., Thomashow, L. (Eds.). Microbial Phenazines: Biosynthesis, Agriculture and Health. Springer. Heidelberg, Germany, pp. 177–198.

Yu, H., He, X., Xie, W., et al. 2014. Elastase LasB of *Pseudomonas aeruginosa* promotes biofilm formation partly through rhamnolipid-mediated regulation. Can. J. Microbiol. 60: 227–235. doi.org/10.1139/cjm-2013-0667

Zohara, F., Akanda, M.A.M., Paul, N.C., Rahman, M., Islam, M.T. 2016. Inhibitory effect of *Pseudomonas* spp. on plant pathogen *Phytophthora capsica in vitro* and in planta. Biocatal. Agric. Biotechnol. 5: 69–77. doi.org/10.1016/j.bcab.2015.12.009